Electromagnetic Modeling Using COMSOL of Field-Emitter Cathodes Inside an L-Band Radiofrequency Gun at Fermilab

H. Panuganti[1,2,3,*] and P. Piot[1,3]
1. Northern Illinois Center for Accelerator and Detector Development (NICADD), Northern Illinois University, DeKalb, IL 60115.
2. Department of Mechanical Engineering, Northern Illinois University, DeKalb, IL 60115.
3. Fermi National Accelerator Laboratory (FNAL), Batavia, IL 60510.
*harsha.panuganti@gmail.com

Abstract: Field-emitter (FE) electron sources offer significant advantages over photocathode and thermionic sources due to their ability to be operated without the need for an auxiliary laser system or a heating source. While FE cathodes have been traditionally used in DC environments, we explore electron beam generation from carbon based FE cathodes inside an L-band radiofrequency (RF) gun at Fermilab, where significantly higher current electron beams are possible owing to high extraction RF electric fields (nominal) on the order of tens of MV/m. In this regard, we present electromagnetic modeling using COMSOL®'s RF module, of the RF gun to understand the electric field profile, eigenfrequencies and field enhancement at the FE tips inside the gun. The field profile and eigenfrequency variation with respect to the considered cathode geometries and position offsets, along with Q-factor studies are presented. Some of the numerical results are compared, where possible, to experimental measurements for validation. Finally, we briefly discuss the future implications of the current work with regards to integration with dedicated charged particle tracing programs and possible multiphysics studies.

Keywords: radiofrequency gun, radiofrequency engineering, field-emitter cathodes.

Introduction

Field emission is an electron emission process where the emission occurs through the quantum mechanical process of tunneling. Considerable number of electrons from a material can tunnel through the surface–vacuum barrier if there are strong (normal) electric fields present at the surface.

Strong electric fields are difficult to generate, but field emission is enhanced by surface roughness. For instance, a sharp feature at the surface will locally increase the field in a similar effect as in the case of a lightning rod. If the electron emitting material has sharp features on its surface, then a macroscopic electric field of magnitude E around the surface is enhanced to a field of $E_e = \beta_e E$ around the sharp feature, where $\beta_e > 1$ is often referred to as the field enhancement factor that depends on the curvature of the tip. The smaller the curvature of the tip, the higher is β_e. Fowler-Northeim (FN) theory predicts the amplitude of the local current I from an emitter to be [1]

$$I = Aj = Aa(\phi)E_e^2 \exp\left(\frac{b(\phi)}{E_e}\right), \qquad (1)$$

where A is the effective area of emission, j is the current density, and a and b are functions of the work function of the material ϕ, with image-charge correction.

In terms of beam quality, FE cathodes can generate electron beams with low emittance and high average current. Electron beams with near quantum-limited transverse emittance can be produced via extremely small FE tips like carbon nanotube (CNT) and diamond [2]. Examples of applications of FEs can be found in THz vacuum electron sources [3], high resolution x-ray imaging which requires high current density electron beams [4].

Field-emitter arrays (FEA) are fabricated by arranging FEs in an orderly fashion as large arrays, thus can provide high average [5] and uniform currents making them ideal for most applications, e.g. in field emission displays (FEDs) [6, 7]. Diamond FEAs, in particular, have applications in free electron lasers as they are rugged and generate little heat [8, 9]. CNT emitters (patterned or randomly oriented) can generate substantial enhancement factors of more than 1000 [10]. These geometric properties coupled with low electrical resistance, high thermal stability and robustness at high temperatures can support large current densities making CNTs excellent FEs.

Most of the research done on FEs so far dwells around studies done in DC fields where the beam energy is limited by low accelerating voltage on the order of a few MV/m at most. In the current proceeding, we report the electromagnetic modeling of an L-band RF gun with regards to FE cathodes,

which can produce substantially higher accelerating gradients, on the order of tens of MV/m, when compared to DC electron guns. Consequently, high energy and high average current electron beams can be generated from FEs using RF fields. Particularly, we report RF gun studies regarding a diamond field emission array (DFEA) cathode and a CNT cathode utilizing the L-band (1.3 GHz) RF gun at the currently decommissioned high-brightness electron source laboratory (HBESL) at Fermilab.

Cathodes Utilized in the Experiment

In this experiment, a DFEA cathode was tested in HBESL's RF gun. The DFEA cathode has $\sim 10^6$diamond tips on their respective pyramids and was synthesized at Vanderbilt University (VU), Tenn. The DFEA diamond tips on the pyramids were deposited on a circular area of 6 mm radius and are approximately separated from one another by 10 µm distance. The typical pyramid base is ~ 4 µm and the radius of curvature of the tip is ~ 10 nm. A scanning electron microscope (SEM) photograph of the DFEA pattern is shown in Fig. 1, while the cathode plug that inserts into the RF gun is shown in Fig. 2. The array was prepared using an inverse mold-transfer process [9].

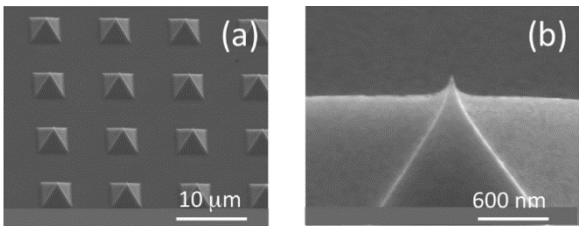

Figure 1: An SEM image of the DFEA pattern (a) and an SEM image of a single tip (b). Image courtesy of Bo Choi (Vanderbilt University).

Figure 2: A photograph of the DFEA cathode brazed on an HBESL cathode. The emitter area is the dark circular area on the plug surface.

A second type of cathode, carbon nanotube (CNT), was also tested in the RF gun. Unlike the DFEA cathode which is an array of diamond FEs, the CNT cathode(s) used for the current experiment is an agglomeration of randomly oriented multi-walled carbon nanotubes (MWCNTs) having sharp tips of about a few nanometer radii. Such a nanotube offers an enhancement factor on the order of $\beta_e \sim 100 - 1000$, much higher than that of a DFEA tip. Two CNT cathodes were tested in the current experiment viz. the 'large' cathode and the 'small' cathode. The large cathode has a molybdenum substrate and consists of a 15-mm diameter CNT emitter area, while the small cathode has stainless steel substrate and consists of a 1.5-mm diameter emitter area [see Fig. 3 (b) and (c)]. The CNT cathodes were synthesized using an electrophoretic deposition (EPD) process, which is a rapid and economical way of producing CNTs with varying properties in large numbers [11]. An SEM image with 20k magnification of the large CNT cathode is shown in Fig. 3 (a). The small cathode was also synthesized using an EPD process by a commercial industry but the process-specifications are unavailable. The small cathode has a different geometry (see Fig. 3 (c)) from the large cathode (see Fig. 3 (b)), as a result of being synthesized at a different facility. A bossed structure of a size of approximately 2-mm diameter and 1.5-mm outward protuberance can be seen on the small cathode.

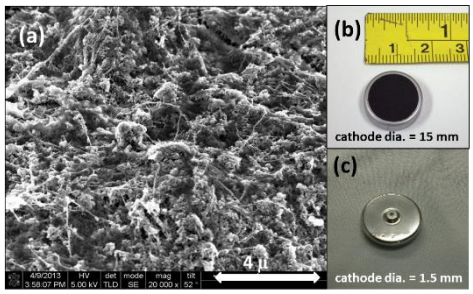

Figure 3: An SEM image of the large CNT cathode with a magnification of 20k showing CNTs and other structures (a), a picture of the large CNT cathode (b), and a picture of the small CNT cathode (c).

Electromagnetic Modeling Pertaining to the DFEA Cathode

Finite element method (FEM) simulations using COMSOL®'s RF module were performed to estimate the field enhancement factor β_e and the longitudinal electric field profile near one DFEA tip. The simulations were also useful to estimate the tolerances on the longitudinal displacement of the cathode from the nominal position inside the gun.

An RF gun model was created with the dimensions of the HBESL gun, derived from a computer-aided drawing shown in Fig. 4. We are interested in the TM_{010} modes of the gun viz. the

zero- and the π-modes, which have cylindrically symmetric electromagnetic fields if we assume the effect of the input coupler to be negligible. Hence only quarter of the gun was modeled as shown in Fig. 5 to conserve computational time, with the appropriate material assignments and boundary conditions specified in Table 1.

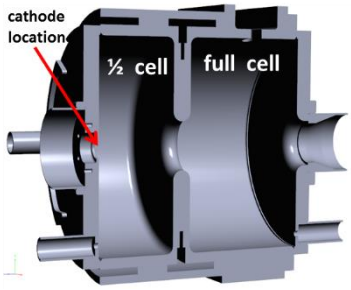

Figure 4: A 3D computer aided drawing (CAD) half-sectional view of HBESL's RF gun, obtained using SOLIDWORKS®.

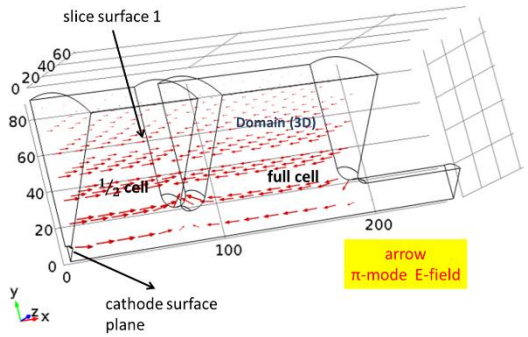

Figure 5: A Finite element model of the HBESL RF (quarter) gun. The distances shown are in mm.

Table 1: Important specifications of the finite element modeling of the RF gun.

Object/parameter	Assignment
slice surfaces 1 & 2	perfect magnetic conductor ($\mathbf{n} \times \mathbf{H} = 0$)
all other surfaces	perfect electric conductor ($\mathbf{n} \times \mathbf{E} = 0$)
domain volume material	vacuum ($\epsilon_r = 1, \mu_r = 1$)
parametric surface	cathode plane
eigenfrequency solving neighborhood	1.3 GHz
n = surface normal vector, **H** = magnetic field intensity, **E** = electric field, _ϵ_r = relative permittivity, μ_r = relative permeability.	

Assigning the slice surfaces (see Fig. 5) the boundary condition (BC) of perfect magnetic conductor makes the problem equivalent to that of having the full gun (when solving for the zero- and the π-modes). All other surfaces were idealized with perfect electric conductor BC for simplicity and to avoid complex electric field/eigenfrequency solutions. The longitudinal position of the cathode surface plane, of size 8.29-mm radius, was parametrized to obtain solution to the first approximation when the cathode is displaced from the nominal position by a known amount. With the conditions specified in Table 1, the following equation was solved in the entire spatial domain (3D) using the default eigenvalue solver available in COMSOL.

$$\nabla \times \mu_r^{-1}(\nabla \times \mathbf{E}) = k_0^2(\epsilon_r - \frac{i\sigma}{\omega\epsilon_0})\mathbf{E}, \qquad (2)$$

where k_0 is the wave number, ω is the angular eigenfrequency, $i = \sqrt{-1}$, and σ is the electrical conductivity. The electric field vector of the π-mode is plotted in Fig. 5 (arrow). In order to get a well balanced peak electric field magnitude in both the $\frac{1}{2}$ cell and the full cell of the gun, the radii of both cells are tuned within a micron. The final axial electric field along the gun's axis is shown in Fig. 6.

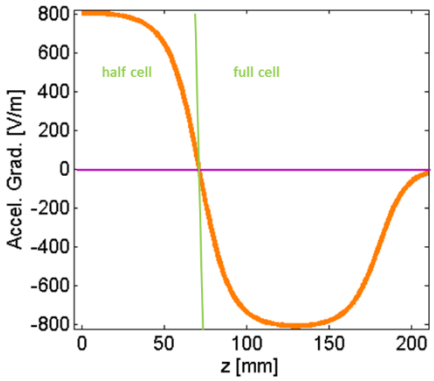

Figure 6: Accelerating gradient (electric field) of the π-mode along the gun when the field is positive at the cathode center, for an arbitrary peak electric field.

For the given geometry of the RF gun, the eigenfrequency of the π-mode is obtained to be 1.298686 GHz. Figure 7 shows how displacing the cathode longitudinally affects the eigenfrequency of the π-mode and the peak electric field on the cathode surface. Correspondingly, Fig. 8 shows how the field profile is perturbed from the nominal case, for different cathode displacements. It can be noted that for the nominal cathode position (cathode displacement set to 0), the default arbitrary peak

electric field is ~810 V/m. This value can be normalized to any desired peak field. For a case of cathode displacement of ~ -2 mm, the FEM simulations suggest a 22% decrease in the peak electric field from 810 V/m to 630 V/m, which forms a basis for experimental tolerances with regards to the cathode's nominal position.

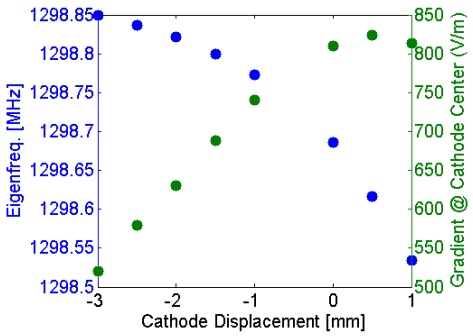

Figure 7: Effect of the cathode displacement on the π-mode eigenfrequency and the peak electric field on the cathode surface. The positive displacement is towards the full cell.

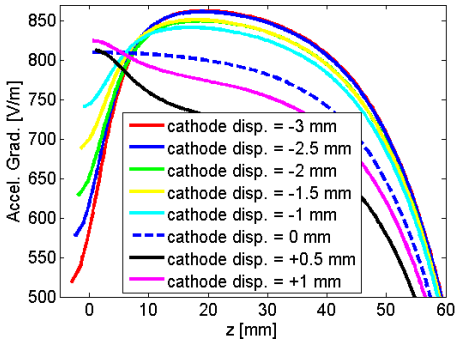

Figure 8: The accelerating gradient profiles near the cathode for the cathode displacements considered in Fig. 7.

A tip of 10-nm radius was introduced on the cathode surface to obtain the field enhancement factor and the enhancement profile. The 10-nm hemispherical tip was integrated to the square face of a pyramid whose size was chosen $4 \times 4 \times 5$ $(\mu m)^3$ to be dimensionally close to an actual DFEA tip used in the experiment. As a result of the introduction of the tip (perfect electric conductor BC), the electric field in the immediate neighborhood of the tip is enhanced from otherwise 810 V/m to ~ 55680 V/m, suggesting an enhancement factor $\beta_e \sim 69$ (i.e $\frac{55680}{810}$); see Fig. 9. Further refinement of the meshing would improve the resolution around the tip, and hence would give higher enhancement factors; but this would considerably increase the requirements on the computing power and computational time. A challenge in introducing a nano-sized tip in a gun whose size is of several hundreds of centimeters is about the mesh adaptation; the volume around the tip requires a much higher mesh resolution than that of the bulk of the gun. Hence in this model, three different sub-domains were created whose mesh element size limits were separately set. At the intersection of these sub-domain surfaces, the default adaptive mesh control was used.

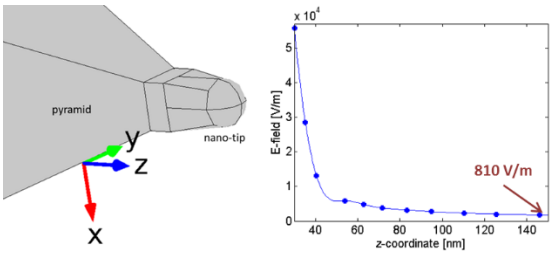

Figure 9: The 10-nm radius tip on a pyramid introduced on the cathode surface (left) and the field enhancement profile in the neighborhood of the tip (right).

Electromagnetic Modeling Pertaining to the CNT Cathodes

Geometrical differences between two cathodes shown in Fig. 3 (b) and (c) could have compelling effects on the RF system, e.g, on the RF power sustained inside a resonating cavity and the maximum electric field that can be achieved. We are particularly interested in learning about how the quality factor, a.k.a the Q-factor, of HBESL's gun is effected by the bossed structure of the small cathode. The Q-factor Q_n of a resonator is a dimensionless quantity that is a measure of the ratio of the sustained power to the dissipated power in the resonator at a given frequency of resonance, and is defined as

$$Q_n(f) = 2\pi f \times \frac{E_S}{P_d}, \qquad (3)$$

where f [Hz] is the resonating frequency of interest, E_S is the time-averaged stored energy [J] inside the RF resonator (gun) at frequency f, and P_d is the dissipated power [W] at frequency f.

The COMSOL model of HBESL gun described in the previous section was utilized and extended for the current study. Here, the gun's geometric model was modeled with the parameter assignments specified in Table 1 except for the perfect metallic conductor BC, which was changed to the finite conductivity metallic conductor of copper. By doing so, an estimation of the Q-factor of HBESL's RF gun could be made since it is made of copper. The conductivity of copper was taken to be 5.96×10^7 S/m (input). In COMSOL, after executing the simulation computation, the time-averaged energy density E_S [W/m^3] and the surface

loss density P_d [W/m^2] are written to file. Thus, the Q-factor can be computed by performing the following numerical integration of

$$Q_n(f) = 2\pi f \times \frac{\int_V E_S(V)dV}{\int_S P_d(S)dS}, \quad (4)$$

where the volume V corresponds to the entire volume of the gun and the surface S corresponds to all the outer surfaces (excluding the internal slice surfaces) of the gun's geometry shown in Fig. 5; both V and S are user-specified via COMSOL's graphic user interface (GUI) while the above equation is user-specified as a mathematical definition that is to be numerically computed.

The estimation of the Q-factor for the case of small cathode was performed in a similar way described above, but the geometry of the gun was modified accordingly by introducing a bossed structure as seen in Fig. 3 (c). The results of the computed Q-factors that are summarized in Table 2 reveal that the geometry of the small cathode does not make any significant difference from the standpoint of the RF system, since the Q-factors for both gun (cathode) geometries are within ~ 0.15 %. The Q-factor computed for the case of nominal geometry (large cathode) agrees with previously performed experimental Q-factor estimation within a few percent. Figure 10 compares the surface resistive loses showing only little difference between the two geometrical cases of the gun.

Table 2: Numerical results of computations of Q-factors of HBESL's RF gun for the cases of large and small cathodes.

Case 1: large cathode (nominal)		
Mode	**Eigenfrequency**	**Q-factor**
π	1.29866e9+i27524.53768	23590.92537
zero	1.29597e9+i29099.37368	22267.94858
Case 2: small cathode		
π	1.29865e9+i27483.2008	23626.16946
zero	1.29594e9+i29140.1135	22236.44309

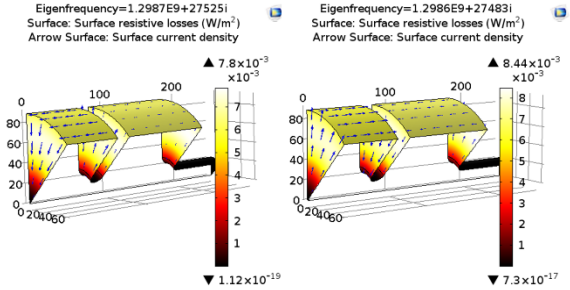

Figure 10: Comparison of surface resistive loses for the two cases of the large (left) and small cathodes (right) in RF gun's π-mode. Note: the maximum electric field in the cavity in the model is arbitrarily scaled to ~ 810 V/m.

To supplement and validate the numerical results on Q-factors, a set of network analyzer and spectrum analyzer measurements were performed on the RF gun for the two cases of nominal and small cathode geometries. A network analyzer measures the tune, or the resonant frequencies of a cavity in a given frequency range by sending a test power to the cavity. A spectrum analyzer measures the frequencies sustained inside a cavity during the designed operation of the cavity i.e when the cavity is powered by the klystron. The spectrum and network analyzer measurements compared in Fig. 11 for the two cases of nominal and small cathodes show no notable differences in the resonant frequencies of the gun, in agreement with numerical results presented in Table 2. The intermodal frequency separation between the zero- and π-modes in Fig. 11 is ~ 2.52 MHz, in agreement with the simulations (2.69 MHz).

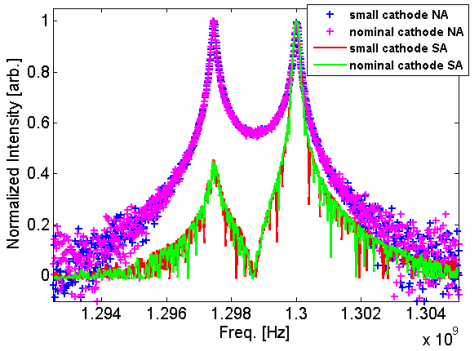

Figure 11: Comparison of spectrum and network analyzer measurements of HBESL's RF gun for the cases of small and nominal (flat) cathodes. NA stands for network analyzer and SA stands for spectrum analyzer. The peaks correspond to the zero- (left) and the π-mode (right) respectively.

Importing Data for Charged Particle Tracing Programs

While GUI based multiphysics softwares like COMSOL have wide applications across various scientific fields, they have some limitations. For instance, in the field of charged particle beam physics, the use of COMSOL currently has not been shown to be competitive with dedicated charged particle tracing programs. The reasons may be attributed to the number of particles that can be simulated, the ease of accommodating electromagnetic elements etc. While advances in the field of GUI based programs continue, one can attempt to integrate the results between programs of distinct kinds. Here, we show an instance of how the

electric fields generated in COMSOL can be served as an input to a dedicated charged particle tracing program called ASTRA (a space charge tracking algorithm), a popular Fortran based program developed at DESY, Germany.

In Fig. 12 the electric field distribution on a DFEA tip, obtained from COMSOL, has been converted to an FN current density distribution using Eq. 1 in MATLAB® at 198 points on the tip. The corresponding electron charge density distribution at 198 locations on the tip was utilized to trace the electrons using ASTRA, as the electrons propagate through a particle accelerator across various electromagnetic elements.

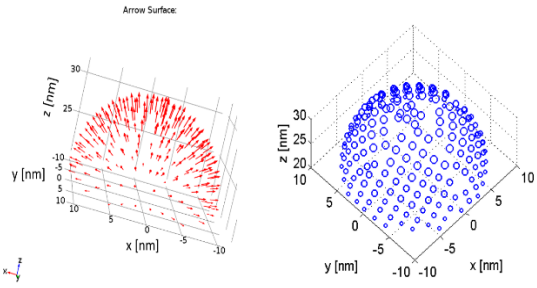

Figure 12: A scatter plot of an FN charge density distribution (right) on the nanotip corresponding to the electric field distribution (COMSOL) represented in the left figure, for an arbitrary total current. The size of a marker represents the magnitude of the current density at the corresponding location.

Figure 13 shows the results from ASTRA regarding some important electron beam parameters corresponding to the HBESL photoinjector beamline. More details regarding the electron beam simulations can be found in Ref. 12. The experimental beam properties and current stability studies can be found in Ref. 13 – 14.

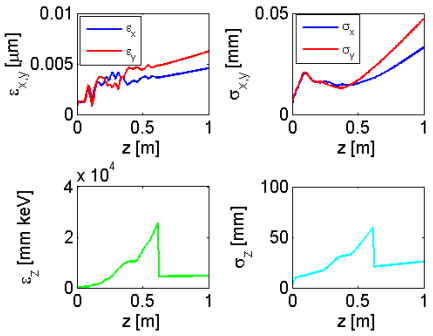

Figure 13: Evolution of transverse (x, y) and longitudinal (z) normalized emittance (ϵ) and rms beam size (σ) of the beam emitted from a single DFEA nanotip, along the HBESL photoinjector beamline, as simulated using ASTRA.

Summary

In summary, we have realized electromagnetic modeling of an L-band RF gun using COMSOL. The studies include estimation of electric field enhancement for a 20-nm diameter nanotip, and field variation with respect to different cathode geometries and cathode position offsets from the nominal position. Additionally, Q-factors and surface heat profiles of the gun were computed corresponding to two cathode geometries considered for the FE experiment. An FN charge density distribution on an FE tip surface was generated using MATLAB upon utilizing the corresponding electric field distribution obtained from COMSOL; this charge density distribution was later utilized for simulation of electron beam properties using a popular charged particle tracing program, ASTRA.

Future Implications

While softwares like COMSOL offer a high level of customization with regards to numerical analysis and multiphysics environment, a one-stop program may not exist to solve some current technological problems. An exciting direction, to take on increasingly complicated problems, appears to be the integration of software programs of distinct kinds to work with one another in an automated way, to arrive at an optimum solution. For instance, complex electron gun geometries may not be modeled in COMSOL, nor is COMSOL's charged particle tracing seems to be competitive with programs like ASTRA in the field of beam physics. However, by taking advantage of LiveLink™ environments in COMSOL, one can attempt to integrate a dedicated CAD program like SOLIDWORKS and a computational program like MATLAB to control the input and output data of ASTRA. If such a scenario can be automated using existing features of the distinct programs involved, while optimizing for a mathematically defined parameter—e.g. optimizing beam emittance with respect to the RF gun/cathode geometry—then such a model may achieve a new level of design optimization.

Funding Source

This work was supported by the U.S. Department of Energy (DOE) under Contract No. DE-FG02-08ER41532 with Northern Illinois University. Fermilab is operated by the Fermi Research Alliance, LLC under Contract No. DE-AC02-07CH11359 with the U.S. DOE.

References

1. R. H. Fowler, L. Nordheim. *Proc. Roy. Soc. of London*, **A 119**, 173 (1928).
2. J. D. Jarvis et al., Resonant tunneling and extreme brightness from diamond field emitters and carbon nanotubes, *J. of Appl. Phy.*, **108**, 094322 (2010).
3. A. Mustonen et al., Five picocoulomb electron bunch generation by ultrafast laser-induced field emission from metallic nano-tip arrays. *Appl. Phys. Lett*., **99**, 103504 (2011).
4. X. Caldern-Coln et al., A carbon nanotube field emission cathode with high current density and long-term stability, *Nanotechnology*, **20**, 32570 (2009).
5. K. B. K. Teo et al., Microwave devices: Carbon nanotubes as cold cathodes., *Nature*, **437**, 968 (2005).
6. G. Fursey, Field Emission in Vacuum microelectronics. *Kluwer Academic/Plenum Publishers*, NY (2005).
7. L. F. Velasquez-Garcia et al., Uniform High Current Cathodes Using Massive Arrays of Si Field Emitters Individually Controlled by Vertical Si Ungated FETs Part 1: Device Design and Simulation, *IEEE Transactions on Electron Devices*, **58**, 6, (2011).
8. C. A. Brau, High-brightness electron beams -- small free-electron lasers, *Nucl. Instr. and Met. in Phys. Res. Sec. A: Accelerators, Spectrometers, Detectors and Associated Equipment*, **407**, 1 (1998).
9. J. D. Jarvis et al., Fabrication of Diamond Field-Emitter-Array Cathodes for Free-Electron Lasers, *Proc. of FEL08*, Gyeongju, Korea (2008).
10. W. Zhu et al., Large current density from carbon nanotube field emitters, *Appl. Phys. Lett*., **75**, 873 (1999).
11. J. J. Hartzell et al., Continued Development and Testing of Carbon Nanotube Cathodes at Radiabeam, *Proc. of NAPAC*, Pasadena, CA (2013).
12. H. Panuganti, Investigations and Applications of Field- and Photo-emitted Electron Beams from a Radio Frequency Gun, *Doctoral Dissertation in Physics*, Northern Illinois University (2015).
13. P. Piot et al., Operation of an ungated diamond field-emission array cathode in a L-band radiofrequency electron source, *Appl. Phys. Lett*., **104**, 263504 (2014).
14. D. Mihalcea, Measurement of Ampère-class pulsed electron beams via field emission from carbon-nanotube cathodes in a radiofrequency gun, *Appl. Phys. Lett*., **107**, 033502 (2015).